Hindawi
Journal of Electrical and Computer Engineering
Volume 2019, Article ID 2450191, 6 pages
https://doi.org/10.1155/2019/2450191

Research Article

Stationary Time Statistical Property of Ionospheric Clutter in High-Frequency Surface-Wave Radar

Shang Shang [1,2] Kangning He [1] Zhaobin Wang [1,2] and Xuguang Yang [3]

[1] *School of Electronics and Information, Jiangsu University of Science and Technology, Zhenjiang 212003, China*
[2] *School of Electronic and Electrical Engineering, University of Leeds, Leeds LS2 9JT, UK*
[3] *School of Information Engineering, Long Dong University, Qingyang 745000, China*

Correspondence should be addressed to Shang Shang; shangshang@just.edu.cn and Zhaobin Wang; wangzb@just.edu.cn

Received 22 July 2019; Accepted 17 September 2019; Published 3 November 2019

Academic Editor: Jit S. Mandeep

In HFSWR (high-frequency surface-wave radar) system, the detection performance is impacted seriously by ionospheric clutter. Frequency selection is an effective method to avoid the effect of ionospheric clutter. The key to the method is the stationarity of ionospheric clutter over a period of time. This paper mainly researches the stationary time statistical property of the ionospheric clutter. A large number of real data including ionospheric clutter in HFSWR are processed and analyzed. It shows that ionospheric clutter in HFSWR has the characteristics of approximate stationarity within a period of time.

1. Introduction

HFSWR is used to achieve overhorizon detection of surface ships and ultralow altitude aircraft by the electromagnetic wave characteristics in which high-frequency band (3–15 MHz) vertical polarization electromagnetic wave spreads along the sea surface [1–3]. HFSWR is considered to be a major technical means to achieve coastal state control and supervision of the offshore exclusive economic zone. HFSWR is regarded as perfect early warning radar. Nowadays, many military and civil fields adopted HFSWR, such as coastal surveillance and early warning, sea-state remote sensing [4], ocean surface pollution monitoring, marine environment monitoring, and resource development [5].

However, HFSWR is inevitably affected by ionospheric clutter, sea clutter, radio interference, and other industrial interference. The ionospheric clutter has many characteristics, such as strong energy, long existence time, covering multiple distance units, and Doppler units. All the targets over 100 km may not be detected when ionospheric clutter is powerful [6, 7]. It has become the bottleneck of HFSWR. Therefore, the study of ionospheric clutter suppression is a focus of research on HFSWR.

The study of ionospheric clutter characteristics is the base of the suppression. The researchers of various countries have researched its signatures from various angles. In [8], the range, Doppler, and direction signatures of ionospheric clutter have been analyzed. The document pointed that the detection range polluted by ionospheric clutter depends on the altitude of ionosphere which reflects electromagnetic waves. The Doppler frequencies of the electromagnetic wave reflected from various layer are different. The Doppler frequencies of E layer ionospheric clutter are low, and those of F layer are relatively higher. Most ionospheric clutters do not have directionality, or the directionality is not strong. In [9], the directionality of ionospheric clutter has been analyzed in detail, and it indicated that ionospheric clutters are divided into two categories, which are specular reflection clutter and spread clutter. Specular reflection clutter affects few Doppler and range cells. Spread clutter takes up more cells. Specular reflection clutters on the same range cell and from different Doppler cells have little similarity directivity. Jiang et al. [10] pointed that ionospheric clutters which take up fewer cells have the same directivity, but clutters which occupy many cells do not have. In [11], the effects of E layer clutter on HFSWR have been analyzed. The paper indicated that the Es clutter changes with the season and time in the Arctic. Time-frequency characteristics of ionospheric clutter are analyzed in [12]. In [13], the statistical properties of clutter intensity, correlation function, etc., have been analyzed. Plasma theory indicated that the reflection of electromagnetic waves on the ionosphere is related to the electromagnetic wave frequency. In other words, ionospheric clutter characteristics are in connection with the frequency. On some frequencies, the effects of ionospheric clutter are serious and even make radar fail to work. But on some other frequency, it will not happen. According to the conclusion, Shang et al. [14] proposed a method, which is used to avoid ionospheric clutter by choosing frequency. But the basis is time stationarity of ionospheric clutter.

According to the above analysis, this paper takes the time statistical characteristics of ionospheric clutter as the research object. First, the ionospheric clutter is preprocessed, and the ionospheric clutter is expressed as a time series. Then, the trend term and stochastic term are separated by wavelet analysis. Finally, a stationary time series analysis is performed on the ionospheric clutter time series.

2. Ionospheric Clutter Time Series Preprocessing

HFSWR adopts an ARD (angle-range-Doppler frequency) spectrum to detect targets. The three-dimensional detection platform is established by the coherent integration and digital beam forming of the time-domain data. As shown in Figure 1, the system works on N frequencies during different integration times. N ARD spectrums can be obtained during NT_s, and T_s is the integration time for each frequency. ARD_i is on frequency f_i, and f_i is one of the alternative frequencies to avoid ionospheric clutter. Time series $\{\text{ARD}_i\}$, $i = 1, 2, \ldots, N$, is obtained by arranging the ARD spectrums in chronological order.

The affected scope in the ARD spectrum and average power of ionospheric clutter are regarded as the index to evaluate the changing situation. V_i represents the number of cells polluted by ionospheric clutter in ith ARD spectrum of the time series $\{\text{ARD}_i\}$. Then, $\mathbf{V}_{\text{IC}} = (V_1, V_2, \ldots, V_N)$ is a time series reflecting the ionospheric clutter pollution scope. Similarly, $\mathbf{P}_{\text{IC}} = (P_1, P_2, \ldots, P_N)$ is a time series on behalf of ionospheric clutter average power, and P_i is the average power of ionospheric clutter in ARD_i. $\mathbf{V}_{\text{IC}}$ and $\mathbf{P}_{\text{IC}}$ are normalized for comparison.

The time series of the affected scope and average power of ionospheric clutter are disturbed by complexity and randomness of ionospheric clutter, together with the environmental noise. Time series $\mathbf{V}_{\text{IC}}$ and $\mathbf{P}_{\text{IC}}$ need preprocessing to eliminate or minimize the effect of disturbance. The series $\mathbf{V}_{\text{IC}}$ ($\mathbf{P}_{\text{IC}}$) can be regarded as nonstationary time series. And $\mathbf{V}_{\text{IC}}$ ($\mathbf{P}_{\text{IC}}$) includes the trend term $\mathbf{V}_d$ ($\mathbf{P}_d$) and the stochastic term $\mathbf{V}_r$ ($\mathbf{P}_r$). They are shown as follows:

$$\begin{aligned} \mathbf{V}_{\text{IC}} &= \mathbf{V}_d + \mathbf{V}_r, \\ \mathbf{P}_{\text{IC}} &= \mathbf{P}_d + \mathbf{P}_r. \end{aligned} \tag{1}$$

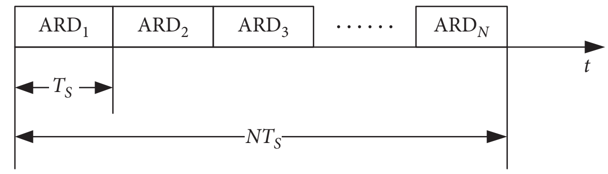

Figure 1: Illustration of ARD spectrum time series.

The trend terms reflect the overall trend of pollution scope and average power of ionospheric clutter. They are the judgment basis of ionospheric clutter to be stationary. The stochastic term reflects the randomness of $\mathbf{V}_{\text{IC}}$ and $\mathbf{P}_{\text{IC}}$, and they are the disturbance factor. Stationary random series analysis and wavelet transformation are adopted to preprocess the time series of the pollution scope and average power of ionospheric clutter, and the trend terms are extracted. Then, the statistical computations of ionospheric clutter approximate stationary time are performed.

2.1. One-Dimensional Wavelet Transform.

Essentially, WT (wavelet transform) analyzes signals by primary function with constantly changing analysis width to realize different resolution ratios in different ranges of frequency [15]. On the basis of multiresolution theory and filter bank theory, the one-dimensional wavelet decomposition is that original signal Y passes through a dual-band bandpass filter group constituted by a high-pass filter and a low-pass filter bank, and high-frequency signal and low-frequency signal are extracted. Then, the low-frequency signal is further decomposed by passing through a dual-band bandpass channel filter, and this process is repeated until the low-frequency signal is decomposed to the mth layer. Signals obtained after the final decomposition are reconstructed by wavelet transform, and the original signal $\mathbf{X}$ can be expressed as

$$\mathbf{X} = \mathbf{L}_m + \mathbf{H}_1 + \mathbf{H}_2 + \cdots + \mathbf{H}_m, \tag{2}$$

where $\mathbf{L}_m$ is the reconstruction result of the mth layer low-frequency signal and $\mathbf{H}_i$ is the reconstruction result of the ith layer high-frequency signal, and $i = 1, 2, \ldots, m$.

During the analysis of ionospheric clutter time series, low-frequency signal reconstruction result $\mathbf{L}_m$ reflects the variation trend as the trend term, and high-frequency signal reconstruction result $\mathbf{H}_1 + \mathbf{H}_2 + \cdots + \mathbf{H}_m$ reflects the interference factors as the stochastic term.

2.2. Stationary Time Series Analysis.

The only way we can regard the high-frequency signal as interference is to guarantee that it is a stable zero-mean random process. That is to say that the random item does not include trend items. So, during the extraction of trend items, it is necessary to take stationarity and zero-mean test.

The common methods adopted for the stationary test include root test, autocorrelation function, partial autocorrelation functions, and parameter test. This paper adopts relatively the objective root test method. The basic idea is to set up time series mode first and then to solve the characteristic root of the characteristic equation established by

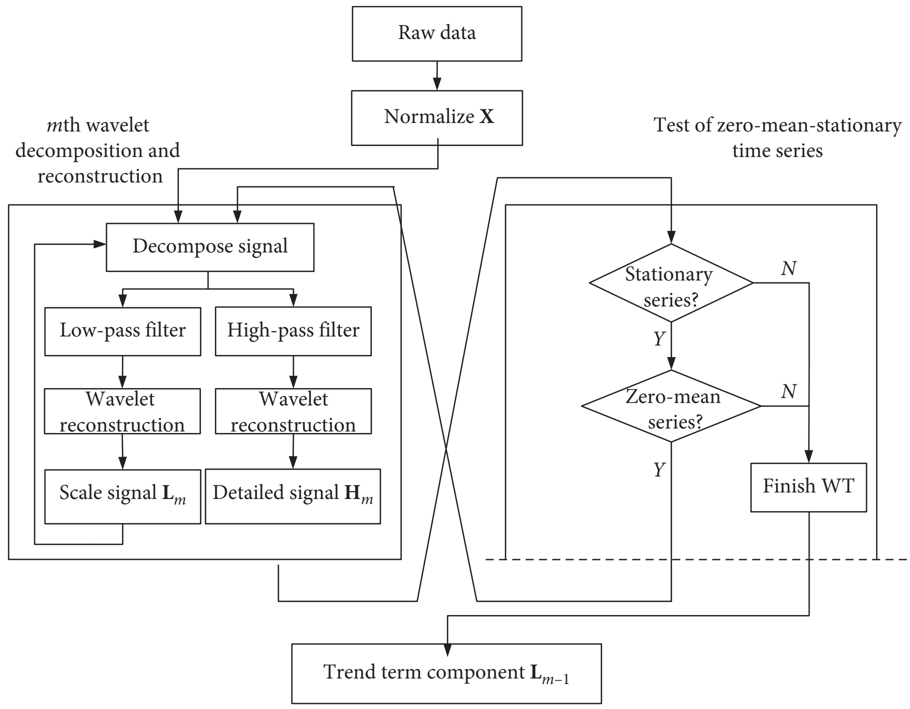

FIGURE 2: Illustration of the trend extraction algorithm.

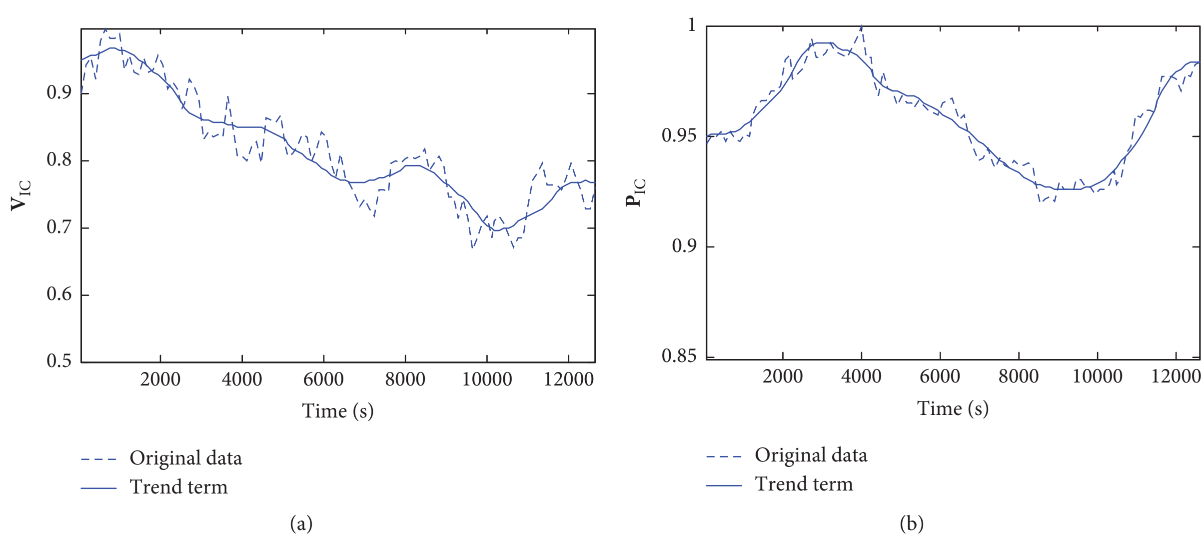

FIGURE 3: Result of trend extraction. (a) Time series $\mathbf{V}_{IC}$. (b) Time series $\mathbf{P}_{IC}$.

the model parameter. Finally, the stationarity of time series is judged by determining whether the characteristic roots are in the unit circle. If all the characteristic toots $\lambda < 1$, that is, mean in unit circle, then the time series is regarded as stationary.

Zero-mean test is the hypothesis testing carried to judge whether the series mean is zero, that is, to test $\mathbf{H}_0$: $\mu = 0$. First variable U is defined as

$$U = \frac{\overline{x} - \mu}{s}\sqrt{n}, \tag{3}$$

where $\overline{x}$ is the mean of the series sample, s is the standard deviation of the series sample, and n is the length of the series sample.

When the hypothesis $\mathbf{H}_0$ is tenable, U approximately subjects to the normal distribution based on the law of large numbers and central-limit theorem. With regard to the confidence level α (here $\alpha = 0.05$), critical value $\mu_{\alpha/2}$ can be obtained by table look-up or calculation. If $|\overline{x} - \mu| \le \mu_{\alpha/2}$, the hypothesis that the mean of the series is zero is accepted.

3. The Algorithm of Trend Term Extraction of Ionospheric Clutter Time Series

$\mathbf{X}$ (here it represents $\mathbf{V}_{IC}$ or $\mathbf{P}_{IC}$) is obtained by real data normalization processing. The purpose of trend term extraction is to eliminate interference composition at most. Trend information should retain integrally. Multilayer wavelet

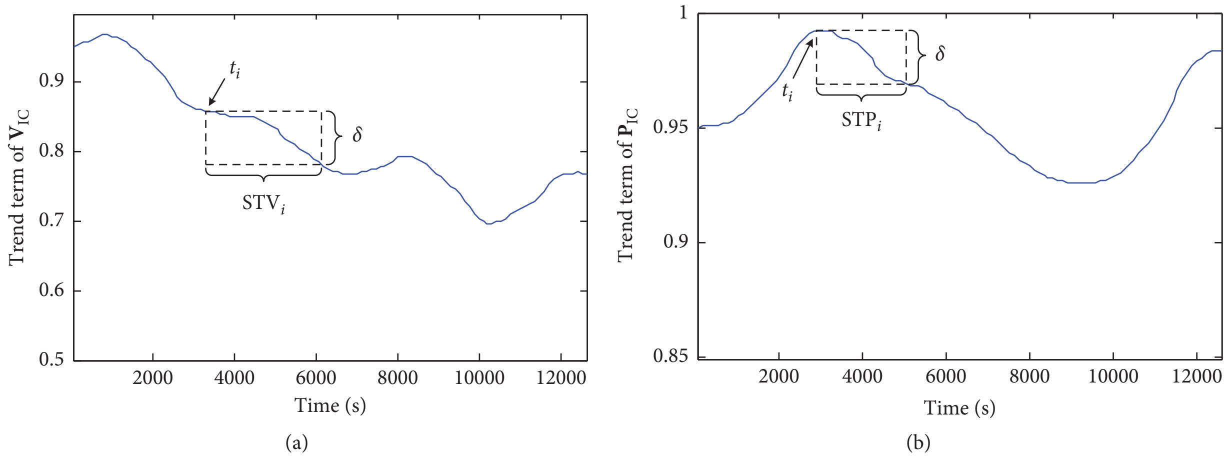

Figure 4: Illustration of ionospheric clutter nearly static time. (a) Nearly static time of $\mathbf{V}_{IC}$. (b) Nearly static time of $\mathbf{P}_{IC}$.

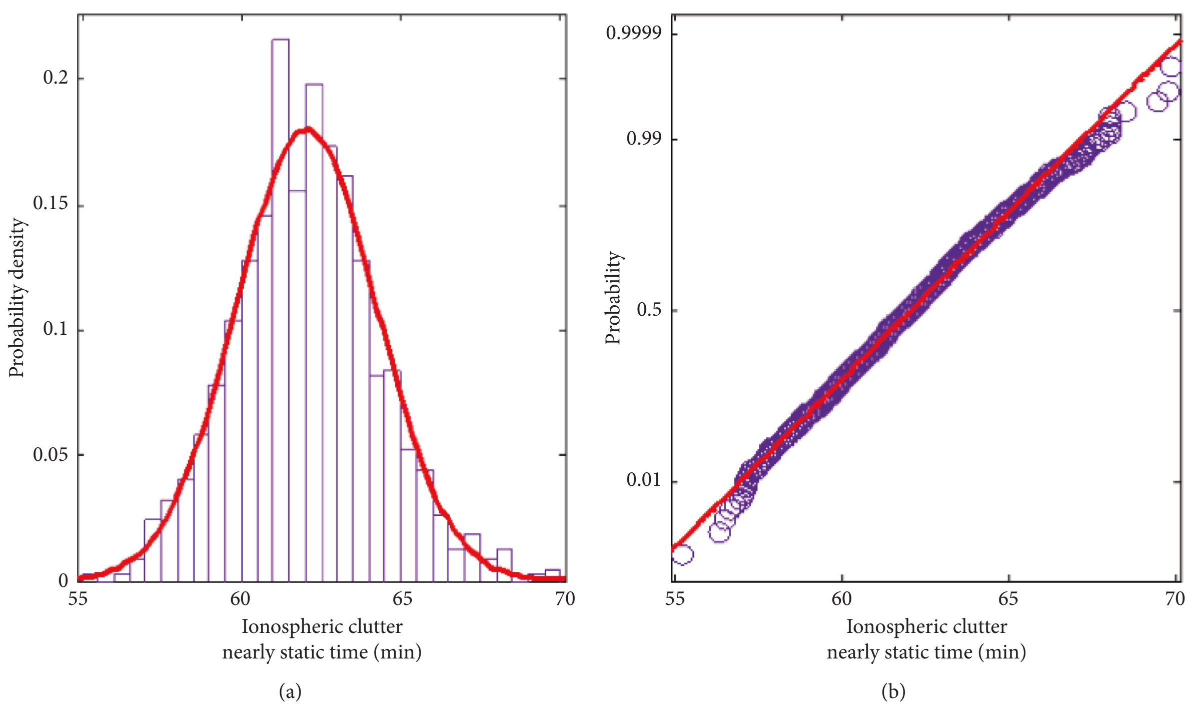

Figure 5: Normality test of ionospheric clutter nearly static time. (a) Density of ionospheric clutter nearly static time. (b) Probability of ionospheric clutter nearly static time.

transform is adopted to decompose $\mathbf{X}$. The layer number of WT is decided by stationary-zero-mean testing for detail signals. Figure 2 shows the concrete flow. The high-frequency signal, which is from the signal decomposition of signal $\mathbf{X}$ by the first layer WT, is tested by stable zero-mean. If the high-frequency signal which stands for the detail is a stable zero-mean series, then the low-frequency signal should be carried on for second time wavelet decomposition. By that analogy, the number of WT is denoted by m when the high-frequency signal dissatisfies stable zero-mean test. The scale signal got from the $(m-1)$th WT decomposition is the trend term.

Take the continuous observation data from 12:35 noon to 15:55 afternoon as example. The coherent integration time $T_{CIT} = 1.9$ min, and ionospheric clutter is identified from the ARD spectrum during the observation time. The scope $\mathbf{V}_{IC}$ and mean power $\mathbf{P}_{IC}$ of normalized ionospheric clutter are shown by the dotted line, and the trend term of them are shown by the solid line in Figures 3(a) and 3(b).

4. The Approximate Stability Time

Ionospheric clutter fluctuates with time. When the affected scope and average power both do not exceed the certain threshold, it is considered approximately stable. The time during which ionospheric clutter keeps an approximate stable station is called the ionospheric clutter approximate stationary time.

The approximate stability time of ionospheric clutter is the time during which the trend terms of normalized ionospheric clutter pollution scope time series $\mathbf{V}_{\mathrm{IC}}$ and average power time series $\mathbf{P}_{\mathrm{IC}}$ both do not exceed the threshold value δ (here $\delta = 0.1$). In Figure 4(a), STV_i denotes the time during which the variability scope of trend term of $\mathbf{V}_{\mathrm{IC}}$ does not exceed δ begin with t_i. In Figure 4(b), STP_i denotes the time during which the variability scope of trend term of $\mathbf{P}_{\mathrm{IC}}$ does not exceed δ begin with t_i. Then, the approximate stability time of ionospheric clutter beginning from t_i $\mathrm{ST}_i = \min\{\mathrm{STV}_i, \mathrm{STP}_i\}$.

During the observation time, the ionospheric clutter stability time beginning with various time periods is shown as histogram in Figure 5(a). The normal fitted curve is drawn on the normal probability paper shown in Figure 5(b), and it is almost a straight line. The approximate stability time of ionospheric clutter conforms to the normal distribution, and the mean value $\mu = 61.02$ min and standard deviation $\sigma = 2.21$ min.

For normal distribution, the ratio that the approximate stability time is within two standard deviations (approximate stability time is within 56.60–65.44 min) is 95.4%. Then, the ratio that the approximate stability time is longer than 56.60 min is bigger than 95.4%. Therefore, for the method to avoid ionospheric clutters by choosing frequency, the ionospheric clutters on various frequencies within 25 min are real-time monitored and the effects on HFSWR are analyzed. The frequency on which the influence of ionospheric clutter is slight is selected, and the result of frequency chosen applies to the next 25 min.

5. Conclusion

Approximate stability property and approximate stationary time of ionospheric clutter are defined based on the analysis of real data of HFSWR, and statistical analysis is performed.

The ionospheric clutter pollution scope and average power time series are preprocessed by stationary time series analysis and WT. The statistical computing of the approximate stability time of ionospheric clutter is taken by the extraction of trend term. The threshold value of ionospheric clutter approximate stability is chosen as $\delta = 0.1$. The analysis of a large number of measured data shows that the rate that the approximate stability time is longer than 56.60 min is larger than 95.4%. It means that on some frequency, ionospheric clutter is approximately stable over 50 min.

It provides the theoretical basis to avoid ionospheric clutter by choosing frequency. According to the analysis results, it is reasonable that ionospheric clutter is monitored and analyzed within 25 min, and it is the basis for choosing frequency during next 25 min.

Data Availability

The data used to support the findings of this study are available from the corresponding author upon request.

Conflicts of Interest

The authors declare that there are no conflicts of interest regarding the publication of this paper.

Authors' Contributions

Shang Shang and Zhaobin Wang contributed equally to this article.

Acknowledgments

The authors express their gratitude for the kind support provided by the National Natural Science Foundation of China (grant nos. 61801196 and 61801141), the Natural Science Foundation of Higher Education Institutions of Jiangsu Province (grant no. 17KJB510014), Jiangsu Government Scholarship for Overseas Studies (grant nos. JS-2018-260 and JS-2018-259), and the Natural Science Foundation of Jiangsu Province of China (grant no. BK20180988).

References

[1] S. Park, C. J. Cho, B. Ku, S. Lee, and H. Ko, "Compact HF surface wave radar data generating simulator for ship detection and tracking," *IEEE Geoscience and Remote Sensing Letters*, vol. 14, no. 6, pp. 969–973, 2017.

[2] C. Yi, Z. Ji, J. Xie, M. Sun, and Y. Li, "Sea clutter suppression method for shipborne high-frequency surface-wave radar," *IET Radar, Sonar & Navigation*, vol. 10, no. 1, pp. 107–113, 2016.

[3] Y. Ji, J. Zhang, Y. Wang, and X. Chu, "Vessel target detection based on fusion range-Doppler image for dual-frequency high-frequency surface wave radar," *IET Radar, Sonar & Navigation*, vol. 10, no. 2, pp. 333–340, 2016.

[4] A. J. Abascal, S. Castanedo, V. Fernández, M. I. Ferrer, and R. Medina, "Oil spill trajectory forecasting and backtracking using surface currents from high-frequency (HF) radar technology," in *Proceedings of the OCEANS 2011 IEEE—Spain*, IEEE, Santander, Spain, June 2011.

[5] J. El Khoury, R. Guinvarc'h, R. Gillard, and B. Uguen, "Simulator of high frequency surface wave radar (HFSWR) with offshore receiver," in *Proceedings of the 2011 IEEE International Symposium on Antennas and Propagation*, IEEE, Spokane, WA, USA, July 2011.

[6] X. Zhang, D. Yao, Q. Yang, Y. Dong, and W. Deng, "Knowledge-based generalized side-lobe canceller for ionospheric clutter suppression in HFSWR," *Remote Sensing*, vol. 10, no. 2, p. 104, 2018.

[7] S. Shang, N. Zhang, and Y. Li, "A new method for ionospheric clutter suppression in HFSWR," in *Proceedings of the 2011 IEEE CIE International Conference on Radar*, IEEE, Chengdu, China, October 2011.

[8] H. C. Chan, "Characterization of ionospheric clutter in HF surface-wave radar," Technical report, Defense Research and Development Canada, Ottawa, Canada, 2003.

[9] X. Wan, X. Xiong, F. Cheng, and H. Ke, "Experimental investigation of directional characteristics for ionospheric clutter in HF surface wave radar," *IET Radar, Sonar & Navigation*, vol. 1, no. 2, pp. 124–130, 2007.

[10] W. Jiang, W. Deng, and J. Shi, "Characteristic study of ionospheric clutter in high-frequency over the horizon surface wave radar," in *Proceedings of the 2009 IEEE Youth Conference on Information, Computing and Telecommunication*, IEEE, Beijing, China, September 2009.

[11] T. Thayaparan and J. Macdougall, "Evaluation of ionospheric sporadic-E clutter in an arctic environment for the assessment

of high-frequency surface-wave radar surveillance," *IEEE Transactions on Geoscience and Remote Sensing*, vol. 43, no. 5, pp. 1180–1188, 2005.

[12] H. Zhou, B. Y. Wen, and S. C. Wu, "Time-frequency characteristics of the ionospheric clutters in high-frequency surface wave radars," *Chinese Journal of Radio Science*, vol. 24, no. 3, pp. 394–398, 2009.

[13] S. Shang, N. Zhang, and Y. Li, "Research of ionospheric clutter statistical properties in HFSWR," *Chinese Journal of Radio Science*, vol. 26, no. 3, pp. 521–527, 2011.

[14] S. Shang, N. Zhang, and Y. Li, "Extraction of ionospheric clutter in HFSWR," in *Proceedings of the 2010 2nd International Conference on Industrial Mechatronics and Automation*, IEEE, Wuhan, China, May 2010.

[15] Z. Wang, S. Shang, G. Zhai, and W. Ren, "Research on storage degradation testing and life prediction based on ARMA and wavelet transform model for aerospace electromagnetic relay," in *Proceedings of the 2014 IEEE 60th Holm Conference on Electrical Contacts (Holm)*, IEEE, New Orleans, LA, USA, October 2014.